EFFECT OF CELLULOSE NANOFIBERS ISOLATED FROM BAMBOO PULP RESIDUE ON VULCANIZED NATURAL RUBBER

P. M. Visakh,[a,b] Sabu Thomas,[b] Kristiina Oksman,[a,c] and Aji P. Mathew*[a,c]

Nanocomposites were prepared using two bioresources, *viz.*, cellulose nanofibers (CNFs) extracted from bamboo paper-pulp waste as the reinforcing phase and natural rubber (NR) as the matrix phase. CNFs with diameters up to 50 nm were isolated from bamboo pulp waste, and nanocomposites with 5 and 10% CNFs were obtained via two-roll mill mixing of solid natural rubber with a master batch containing 20 wt% CNFs. The NR phase was cross-linked using sulphur vulcanization. The morphology studies showed that the dispersion of CNF in NR matrix was not optimal, and some aggregates were visible on the fracture surface. The tensile strength and modulus at 50% elongation increased for the nanocomposites with the addition of CNFs, accompanied by a moderate decrease in elongation at break. The storage modulus of the natural rubber significantly increased above its glass-rubber transition temperature upon nanofiber addition. The addition of CNFs also had a synergistic impact on the thermal stability of natural rubber. The susceptibility to organic solvents decreased significantly for the nanocomposites compared to crosslinked NR, which indicated restriction of polymer chain mobility in the vicinity of the nanosized CNFs in the NR matrix.

*Contact information: a: Wood and Bionanocomposites, Division of Materials Science, Department of Engineering Sciences and Mathematics, Luleå University of Technology, 97187 Luleå, Sweden; b: Centre for Nanoscience and Nanotechnology Mahatma Gandhi University, P. D Hills P.O, Kottayam, Kerlala, India. 686560; c: Composite Centre Sweden, Luleå University of Technology, 97187 Luleå, Sweden
* Corresponding author: aji.mathew@ltu.se*

INTRODUCTION

Elastomeric matrices having relatively low mechanical strength and modulus under room conditions are ideal candidates for reinforcement with cellulosic materials. Fibrous materials have been used in rubber compounds to provide good reinforcement in the past few decades. Short cellulose fibers have been studied extensively in this context (Derringer 1971; Boustany and Hamed 1974; Coran *et al*. 1974; Jacob *et al*. 2004).

Nanocelluloses, which typically have a width of 5 to 50 nm and a high specific surface area, have seen rapid advancement and considerable interest in the last decade owing to their renewable character, advantageous mechanical properties, low density, availability, and diversity of sources (Favier *et al*. 1995; Samir *et al*. 2005; Dufresne 2006; Jonoobi *et al*. 2010; Henriksson *et al*. 2007; Bendahou *et al*. 2009; Bras *et al*. 2010; Siqueira *et al*. 2011). In the recent years, NR-based nanocomposites with biobased nanoreinforcements like nanowhiskers extracted from wheat straw, *Syngonanthus nitens*

(*Capim dourado*), rachis of palm tree, sisal, bagasse, chitin, *etc*. are found in the literature (Hajji *et al*. 1996; Bendahou *et al*. 2009; Siqueira *et al*. 2010, 2011; Bras *et al*. 2010; Nair and Dufresne 2003). Most of these studies deal with natural rubber latex-based nanocomposites prepared by casting and no attempts to develop vulcanized NR-based nanocomposites have been reported. It is also noticeable that relatively few reports are available on cellulose nanofibril-reinforced NR (Phiriyawirut *et al*. 2010; Siqueira *et al*. 2011).

Bamboo fibers are traditionally used in construction and as reinforcing fibers in agricultural and fishing tools, handicrafts, musical instruments, furniture, civil engineering (bridges, scaffolding poles), domestic building (house frames, walls, window frames, roofs, interior dividers), paper, textiles, and board (including rayon, plywood, oriented strand board, laminated flooring) (Scurlock *et al*. 2000). Bamboo fibers are relatively long (1.5 to 3.2 mm) and thus ideal for paper production. Several reports on the out to utilization of native and physically or chemically treated bamboo as reinforcement for composites, are found in the literature (Bao *et al*. 2011; Chen *et al*. 2009)

The present paper reports the extraction of cellulose nanofibers from bamboo pulp production waste and their use as a reinforcing phase in natural rubber (NR). The use of cellulose nanomaterials, which are biobased, as the reinforcing phase in a biobased matrix like natural rubber provides a viable route to extend the applications of natural rubber without compromising on its 'greenness'. The availability of NR in latex form also provides an added processing advantage in terms of dispersion and distribution of nanocellulose in NR, taking advantage of the common suspension medium. The natural rubber and bamboo cellulose nanofiber master-batch was compounded using a two roll mixing mill, and sulphur vulcanization was employed to introduce crosslinks in the NR phase. Vulcanization, a chemical process in which long chains of rubber molecules are cross-linked, transforms the soft, weak plastic-like material into a strong, elastic product with high and reversible deformability and good mechanical properties by strain-induced crystallization, low hysteresis, and excellent dynamic properties and fatigue resistance (Brydson 1978; Hoffman 1967; Aprem *et al*. 2005). After vulcanization, rubber loses its tackiness, becomes insoluble in solvent, and becomes more resistant to heat, light, and the aging processes (Brydson 1978; Hoffman 1967). Different properties of the cellulose nanofibers/NR rubber nanocomposites such as morphology, thermal stability, dynamic mechanical properties, tensile properties, and interaction with organic solvents were studied and reported.

EXPERIMENTAL

Materials

Waste bamboo cellulose pulp was kindly supplied from the Piravam Paper Mill, Kerala, India, and was used as the raw material for the extraction of nanofibrils. Mechanical fibrillation of bamboo waster pulp into cellulose nanofibers was carried out using a super masscolloider (MKCA6-3, Masuko Sanyo Co, Ltd., Japan). The process of mechanical fibrillation is reported in detail in the literature (Visakh *et al*. 2011a). AFM images in Fig. 1 show the size and size distribution for the nanocellulose fibers used in

the study, having diameters between 23 and 42 nm. The length of the cellulose nano-fibrils cannot be estimated from the AFM image, but may be considered to be in the range of several micrometers.
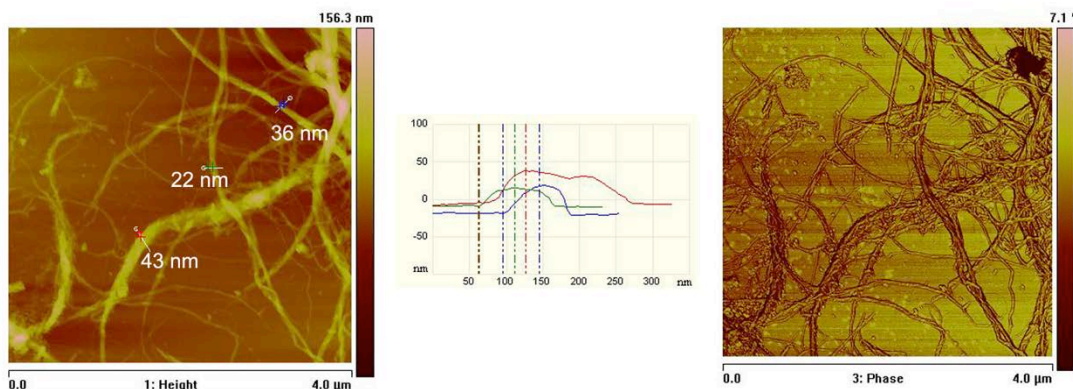

Fig. 1. AFM observation of cellulose nanofibrils showing the height image (left), diameter measurement (middle) and the phase image (right)

Natural rubber (NR) was kindly supplied in latex and solid form by Rubber Research Institute, Kottayam, Kerala, India, and was used as matrix material. The concentration of NR latex used was 97.5%. The used rubber chemicals for vulcanization were purchased from Ceyenar Chemicals Pvt. Ltd. Kottayam, Kerala, India. Toluene was purchased from VWR, Sweden, and was of reagent grade.

Nanocomposite processing

Nanocomposites of cellulose nanofibrils with natural rubber as a matrix were prepared via a two-step process involving a) master-batch preparation in NR latex and b) compounding of the master batch with solid NR and vulcanizing agents using a two-roll mill followed by subsequent curing. The nanocomposite processing was reported in detail in earlier reports on NR-based cellulose nanocomposites (Visakh *et al*. 2012a,b). The resulting nanocomposites had CNF concentrations of 5 and 10 wt% and were coded as NR-CNF$_{5.0}$ and NR-CNF$_{10}$, respectively.

The cure time for the vulcanization was determined using a Monsanto rheometer, and optimum cure times (t_{90}) were calculated and pressed into vulcanised sheets using a compression-moulding machine. The curing of the samples was carried out at 150 °C and 0.5% strain for 30 minutes.

Methods

Scanning electron microscopy (SEM)

The morphological investigations of samples (neat NR and NR-CNF$_5$, NR-CNF$_{10}$) were performed using a Jeol JSM- 6460LV Scanning Electron Microscope (SEM). The specimens were frozen with liquid nitrogen, and fractured samples were used for SEM analysis. Analyses were performed using an acceleration voltage of 15 kV. The materials were sputter-coated with a gold layer to avoid charging.

Dynamic mechanical analysis

Dynamic mechanical measurements such as the logarithm of the storage tensile modulus (E') and loss angle tangent (tanδ) of pure NR, NR-CNF$_5$, and NR-CNF$_{10}$ were carried out with an apparatus DMA D800 from TA Instruments, operating in the tensile mode. The rectangular strips had dimensions of around 40 x 5 x 1 mm^3. Tests were performed under isochronal conditions at 1 Hz and the temperature was varied between -100 and 50 °C by increments of 2 °C. The strain amplitude was limited to 0.05% to be in the linear viscoelastic range of the material.

Tensile mechanical properties

Tensile tests were performed on dumbbell-shaped samples punched from the molded sheets, according to ASTM Standard D 412-97, on an H50KT (Tinius Olsen) Universal Testing Machine with a load cell of 1000 N and crosshead speed of 500 mm/min, using a 4 cm gauge length. The experiments were performed at room temperature. At least five samples were tested for each material and the average values and standard deviations were reported.

Solvent resistance

Solvent interaction with toluene was analysed using gravimetric solvent uptake studies. Circular samples of 1 cm in diameter were cut from the vulcanized sheets by means of a standard circular die. The thickness and initial weight (W_0) of the samples were measured. The thickness of the samples was in the range of 1.5 to 2 mm, and the experiments were conducted under ambient conditions (25 °C). The samples were removed at specific intervals (t) and weighed to the nearest ±0.1 mg using an electronic balance until equilibrium weight (W_∞) was attained. Before each weighing, the surfaces of the samples were cleaned gently without any pressure using filter paper to remove the adhering solvents. The maximum percent uptake of the solvent at different time intervals was calculated using the equation

$$\text{Solvent uptake (wt\%)} = 100 \times (W_\infty - W_0) / W_0 \qquad (1)$$

Thermo gravimetrical analysis

Thermal analyses of cellulose nanofibrils, neat NR, NR-CNF$_5$, and NR-CNF$_{10}$ were carried out using an apparatus TGA D500 from TA Instruments. The scanning range was 30 °C-600 °C, using a heating rate of 10 °C min^{-1} in air for all samples. The DTG curves of the nanocomposites were also reported.

RESULTS AND DISCUSSION

Morphology of Nanocomposites

The examinations of the fractured surface of NR-CNF composites were carried out using SEM, and the images are given in Fig. 2. This technique usually provides information about the homogeneity of the composite, presence of voids, dispersion level

of the nanofibrils within the continuous matrix, presence of aggregates, sedimentation, and possible orientation of nanofibrils.

The images show that the fracture surface was relatively rougher for the nanocomposites, compared to vulcanized NR. Generally, the images show that the cellulose nanofibers were distributed homogeneously with the NR phase, but dispersion on a nanoscale cannot be evaluated at this magnification. The white dots, having different sizes, on the nanocomposites, can be considered as CNF or vulcanizing agents embedded in NR matrix. In the matrix without CNF the dots can be attributed to vulcanizing agents, whereas in the nanocomposites a larger number of white dots are visible. The amount of these smaller white dots was found to increase with increasing CNF content, indicating that these smaller dots were mostly indications of CNF dispersed in NR matrix.
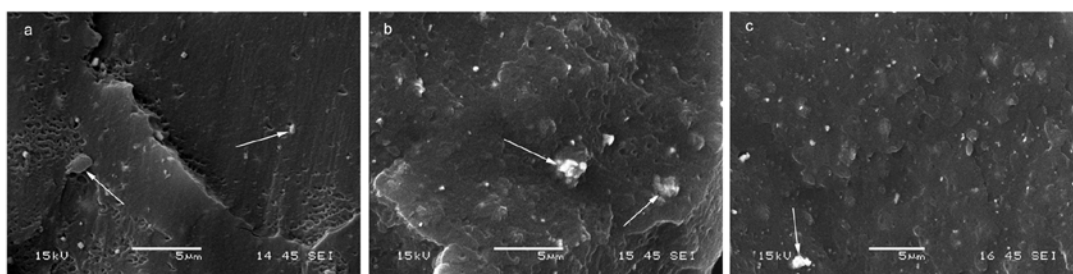

Fig. 2. SEM images of a) Neat NR matrix, b) NR-CNF5, and c) NR-CNF10

The SEM images in this scale showed some microscaled aggregates in the range of 1 micron (marked using arrows). Furthermore, the cross-sections did not show any evidence of sedimentation or concentration gradient, and cellulose nanofibrils seem to be homogeneously distributed in the rubber matrix. Sedimentation of nanoparticles and the development of a concentration gradient is a typical phenomenon observed in solution-casted nanocomposites (Angles and Dufresne 2001; Siqueira *et al*. 2011). Therefore, the processing route used, which involved solution-casting followed by mill-mixing, can be considered as an efficient method to distribute nanocellulosic reinforcements in elasto-meric matrices without a concentration gradient.

Tensile Behavior

Typical stress *vs*. strain curves for the cellulose nanofibrils (CNF)/NR rubber nanocomposites are shown in Fig. 3. It was observed that in all the materials the strain was macroscopically homogeneous and uniform along the sample until its break. The curves show typical behavior for vulcanized rubber, marked by an increase in stress due to strain-induced crystallization at higher strain levels. Apart from the increased stress at break, the general behavior of the curves was not significantly affected by the addition of CNFs. In the current study, the stress-strain curves suggest that the vulcanization or crosslinking of the NR phase, rather than the presence of CNFs, predominates the tensile behavior. A previous study on cross-linked NR reinforced with cellulose nanowhiskers also showed a similar behavior (Visakh *et al*. 2011b).
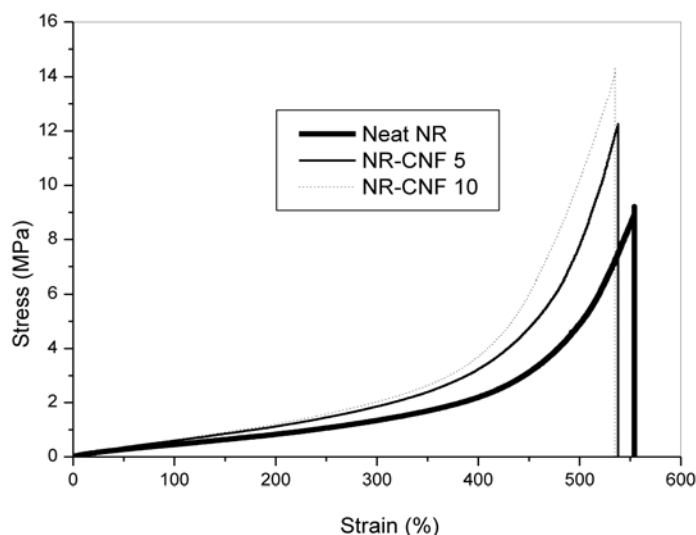
Fig. 3. Stress vs. strain curve of crosslinked NR and NR-CNF nanocomposites

The tensile modulus (at 50% elongation), tensile strength, and elongation at break of the films were determined, and the results are collected in Table 1.

Table 1. Tensile and Dynamic Mechanical Thermal Properties of the Vulcanised NR and its Cellulose Nanocomposites

Samples	Tensile Strength (MPa)	Elongation at break (%)	Modulus @ 50% elongation (MPa)	Storage Modulus 25 °C (MPa)	Tan delta Peak temperature (°C)
NR	9.2± 1.3 (0.56)*	554 ± 9 (576)*	1.7± 0.2 (0.5)*	1.5	-47.5
NR-CNF5	12.3± 1.8 (2.3)*	538± 16 (5.9)*	2.3± 0.3 (102)*	2.2	-45.8
NR-CNF10	143± 1.2	535 ± 13	2.7± 0.2	8.2	-41.3

* literature values from Siqueira *et al.* 2011.

The tensile strength of NR was 9.21 MPa, and it increased to 12.16 MPa and 14.34 MPa with a cellulose nanofibril content of 5 to 10 wt%, respectively. All the nanocomposite materials showed moderate improvements in the tensile modulus as well (1.7 MPa for NR matrix to 2.3 MPa in the case of nanocomposites with 5 wt% CNFs). The modulus NR-CNF$_{10}$ was 2.7 MPa, which corresponds to a two-fold increase compared to neat NR. Table 1 shows the effects of cellulose nanofibrils on the percentage of elongation at break. The percentage of elongation at break decreased with increasing cellulose nanofiber concentration. The elongation of the nanocomposites decreased progressively with the addition of CNFs. NR showed an EB% of 554%, whereas the nanocomposite with 10 wt% CNFs showed an EB% of 535% (Table 1). This decrease was not statistically significant. The improvement in tensile strength and the modulus for

the nanocomposites compared to NR matrix was mainly attributable to the high mechanical properties of CNF compared to matrix. In addition the nanofibers are expected to form entangled network in the NR phase, thereby restricting the matrix mobility.

Some earlier reports have shown significant changes in tensile behavior with the addition of cellulose nanoreinforcements in unvulcanised NR (Bras *et al*. 2010; Siqueira *et al*. 2011). It may be noted that the matrix phase (*i.e*. cross-linked NR) in the current study had a higher tensile strength (9 MPa) and modulus (1.7 MPa) and slightly lower elongation at break (554%) than those reported in earlier studies (see Table 1) (Siqueira *et al*. 2011; Bras *et al*. 2010). This higher strength and modulus of the matrix material in the current study are attributable to the vulcanization (cross-linking) of NR as well as the processing method used. Furthermore, the tensile strength after the addition of 6 wt% nanocellulose was 2.3 MPa, as repored by Sequiera *et al*., which is lower than that found in the current study (12 MPa at 5 wt% CNFs). However, the tensile modulus of NR nanocomposites with 5 wt% bamboo waste-based nanofibers in this study (2.3 MPa) was much lower than that obtained using sisal nanocellulose (102 MPa). Siqueira *et al*. reported a significant drop in elongation at break at 6 wt% MFC content, whereas the elongation at break was not significantly affected by CNF in the current study. The percent change in mechanical properties with the addition of CNFs is not as significant as found in earlier reports on NR-based nanocelulose composites (Bendahou *et al*. 2009; Bras *et al*. 2010; Siqueira *et al*. 2011). This may be attributed to the cross-linking of matrix, which predominates over the influence of nanofibers. However, comparing with cross-linked NR matrix, the nanocomposite containing cellulose nanofibrils showed improvements, both in the tensile strength and modulus with no significant decrease in elongation at break.

Furthermore, comparing the performance of NR-CNF nanocomposites to the recent study on NR-CNW nanocomposites, it was noticed that CNW was slightly more efficient as a reinforcing phase than CNF in cross-linked NR matrix (Visakh *et al*. 2011b). However, the elongation at break was higher for CNF naocomposites, compared to CNW, which is due to the higher aspect ratio of CNFs.

Dynamic Mechanical Properties

Figure 4 shows the DMA analysis plot of log (E'/Pa) (storage tensile modulus) and tan δ (loss angle tangent) at 1Hz as a function of temperature. At low temperatures, the NR was in a glassy state and E' remained roughly constant, around 3×10^9 Pa, due to the fact that in the glassy state, molecular motions are largely restricted to vibration and short-range rotational motions. Though the glassy modulus did not improve with the addition of 5 wt% CNFs (2.1 GPa), an improvement was observed at 10 wt% CNF, being 2.4 GPa for NR and 2.9 GPa for NR-CNF 10. Additionally, it can be seen that the relaxation of polymer chains was delayed for the nanocomposites (at 5 and 10 wt%) compared to NR, resulting in an increased thermal stability in the presence of CNFs (this is also reflected in the positive shift of the tan delta peak position). The storage modulus fell to the region of 1 MPa above the transition region of the curve for NR. In the case of the nanocomposites, the storage modulus above the transition region increased with CNF

addition, especially at 10 wt% CNF (8.2 MPa at 25 °C) compared to NR matrix (1.5 MPa at 25 °C) (See Table 1).

Tan δ exhibited a maximum around -47 °C for NR matrix, and a shift in tan delta position with increasing cellulose nanofibril content (-41 °C) was observed (See Table 1). Moreover, there was a marked decrease in the tan delta peak intensity combined with peak broadening for the nanocomposites with 10 wt% CNFs. The tan delta peak shows the amount of matrix material capable of relaxation, which depends on the concentration of matrix phase and the restriction of chain mobility at the interphase between the matrix and reinforcement. In earlier studies the tan delta peak intensity was found to decrease with the addition of nanoreinforcements even at concentrations as low as 1 wt% (Jonoobi *et al.* 2010). Though in the current study, 5% did not show a decrease in peak intensity, the restriction of chain mobility was evident from the slight positive shift in tan delta peak position at 5 wt% CNF.
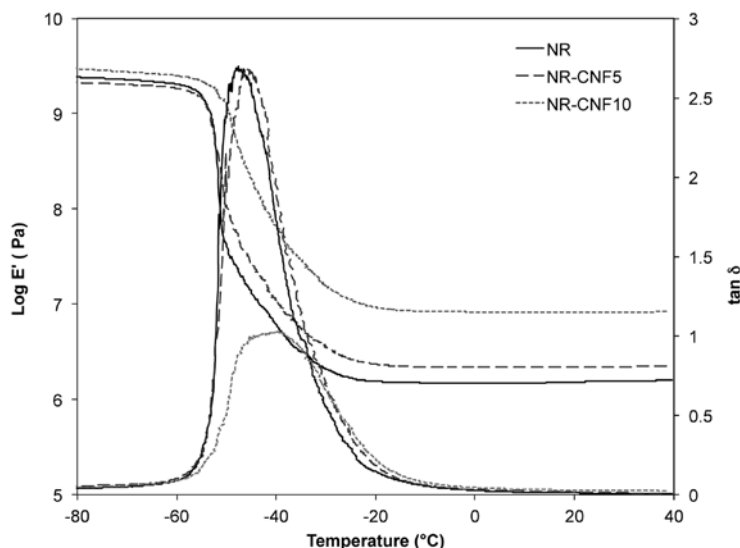

Fig. 4. Dynamic mechanical analysis of neat NR and cellulose nanofiber-based nanocomposites showing the logarithm of the storage tensile modulus (E') and loss angle tangent (tan δ) as a function of temperature

Solvent Uptake Behaviour

Figure 5 shows plots of solvent uptake (weight %) vs. $t^{1/2}$ for the toluene in the NR nanocomposites with different weight percentages of CNFs.

It may be noted that toluene dissolves NR in uncross-linked (unvulcanised) NR materials and cannot be used for swelling studies. In vulcanised NR and its nano-composites, toluene can act as a molecular probe to provide information about the internal structure. All curves in Fig. 5 show a similar pattern with a relatively rapid uptake in the initial stage and a plateau region in the later stage. Two well separated zones were observed at shorter times; zone I, ((time)$^{(1/2)}$ min$^{(1/2)}$ < 15), where a rapid increase in solvent uptake occurs, and zone II ((time)$^{(1/2)}$ min$^{(1/2)}$ >15), where the solvent absorption slows down and equilibrates.
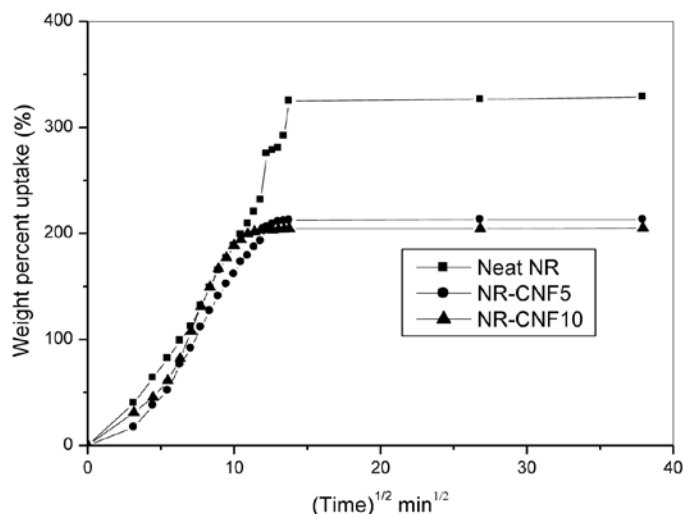
Fig. 5. Solvent uptake behaviour for cross-linked NR and its nanocomposites, immersed in toluene

Table 2 shows the solvent uptake (wt%) of NR and nanocomposites with 5 and 10 wt% CNFs. NR shows an uptake of 328%, which was reduced significantly with the addition of CNFs.

Table 2. Toluene Uptake and Apparent Crosslink Density for Natural Rubber and its Cellulose Nanocomposites

Sample	Equilibrium Weight Percent Uptake (%)	Apparent Crosslink Density
NR	328	0.1904
NR-CNF$_5$	213	0.2275
NR-CNF$_{10}$	205	0.2295

A similar trend of decreasing toluene uptake was observed in NR-based nanocomposites with layered silicates (Varghese and Karger-Kocsis 2003). In layered silicates, the plate-like geometry of the nanoreinforcements is a major factor inducing tortuosity and thereby decreased permeation. In the case of CNF-based nanocomposites, any reduction in the solvent uptake is an indirect measure of the interaction between the matrix and the reinforcements and the presence of interphase where the polymer chain mobility is totally arrested or limited (assuming that the used solvent probe has an affinity only for the matrix and is inert with respect to the nanocellulose). Therefore, in NR-CNF nanocomposites the large interphase due to nanosized morphology of CNFs and the network formation of CNF in NR phase by physical entanglements might be the reason for this behavior. Contrary to this result, Phiriyawirut *et al*. (2010) reported that the water absorption of NR-based nanocomposite films containing cellulose microfibrils was higher compared to pure NR (2010). Similar results were obtained for CNW-reinforced NR in presence of water (Bras *et al*. 2010).

The apparent cross-link densities of the studied materials were determined based on the toluene uptake, and results are shown in Table 2. The volume fraction of the rubber in the swollen gel (V_r) is used to represent the apparent cross-link density and is determined by Eq. 2 (Ellis and Welding 1964),

$$V_r = \frac{1}{1+ (m_b-m_a)/m_a) \cdot \rho_r/\alpha \rho_s)} \qquad (2)$$

where m_a and m_b are the sample mass before and after swelling, ρ_r and ρ_s are the densities of rubber and solvent, respectively, and α is the mass fraction of rubber in the vulcanizates. A higher V_r value indicates a higher degree of cross-linking. Here the values of apparent cross-link densities increased with increased CNF content, which is in agreement with the lower solvent uptake in the presence of CNFs.

Thermal stability and degradation behavior

Neat NR, cellulose nanofibrils, and the nanocomposites having the fibril content of 5% and 10 wt% were used for the TGA analysis, and the results are shown in Fig. 6.
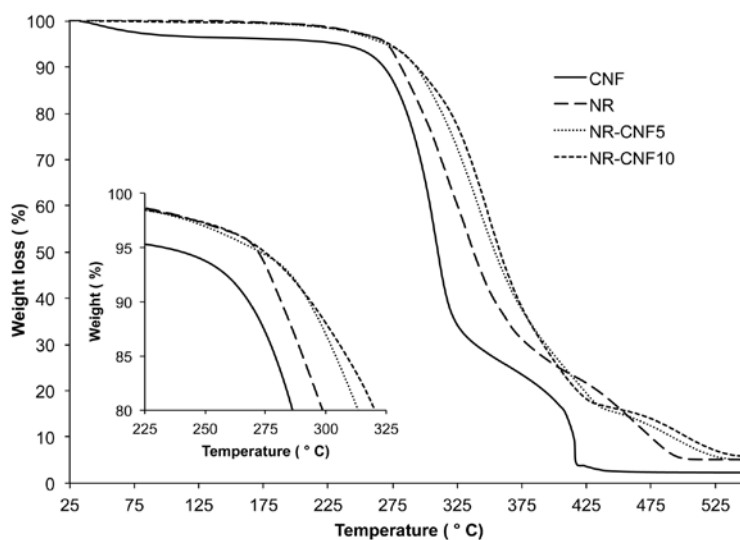

Fig 6. TGA curves of cellulose nanofibrils, cross-linked NR, and NR-CNF nanocomposites showing thermal degradation behavior

The degradation of the cellulose nanofibrils samples involves two main degradation stages, which is typical for cellulose. The onset degradation (T_o) of cellulose is believed to be due to the evolution of non-combustible gases such as carbon dioxide, carbon monoxide, formic acid, and acetic acid, while the second degradation stage is believed to be due to pyrolysis and evolution of combustible gases (LeVan 1989).

In the TGA curves for pure NR and the nanocomposites, multi-step degradation behavior was observed. The initial degradation temperature range of neat NR matrix ranges from 242 to 315 °C, but in the case of NR-CNF$_5$ nanocomposites the degradation temperature range was 268 to 347 °C, and for NR-CNF$_{10}$ it moved up to the range of 271 to 360 °C. Above 400°C the volatile products of degradation are removed. The char

residue obtained by heating above 500 °C was lowest for CNF (2.4 wt%) and was the highest for NR-CNF$_{10}$ (5.64 wt%). The detailed view of onset of degradation is shown in the inset figure. The onset of degradation was around 240° C for CNF and 250° C for NR. For the nanocomposites the value was above 270° C. The results clearly show that the onset of degradation (T_o) shifted to higher temperatures due to the addition of CNF into the NR matrix. The increase in thermal stability when increasing the CNF content from 5 to 10 wt% was, however, not very significant.

The study on thermal degradation showed that the nanocomposites performed synergistically compared to the used matrix and the reinforcement. It is expected that cellulose nanofibers are encapsulated by NR matrix and thereby have a delayed onset of decomposition. The increase of thermal stability for NR by the addition of CNF may be associated with the high amount of interphase with restricted chain mobility generated due to the large surface area of nanocellulose and the entanglement of CNF network. The restricted chain mobility will retard the polymer chain scission as well as escape of byproducts. Similar observations were found in our earlier studies also (Visakh *et al.* 2012b).

CONCLUSIONS

1. Cellulose nanofibrils having a diameter of 23 to 50 nm were successfully prepared from bamboo pulp fibers by mechanical fibrillation and incorporated into natural rubber latex to form a master batch, which was further compounded with solid NR by mill mixing. The NR phase was cross-linked via sulphur vulcanization.
2. The addition of CNFs had a positive impact on tensile strength, modulus and thermal stability, and solvent resistance. Tan delta peak position as well as the degradation onset (T_o) and peak degradation temperature (T_{max}) showed a positive shift for the nanocomposites, compared to the cross-linked matrix.
3. The values of tensile strength obtained (14 MPa) in this study were superior to some earlier reports on NR reinforced with nanocelluloses, which can be attributed more to the vulcanization or cross-linking of matrix phase than the presence of nano-reinforcement.
4. The processing of cross-linked natural rubber-cellulose nanocomposites by master batch preparation followed by two-roll mill compounding, was found to be a viable route to produce mechanically, thermally, and chemically stable nanocomposites.

ACKNOWLEDGMENTS

REFERENCES CITED

Aprem, A. S., Joseph, K., and Thomas, S. (2005). "Recent developments in the crosslinking of elastomers," *Rubber Chemistry and Technology* 78(3), 458-488.

Angles, M. N., and Dufresne, A. (2001), "Plasticized starch/tunicin whiskers nanocomposite materials. 2. Mechanical behavior," *Macromolecules* 34, 2921-2931.

Bao, L., Chen, Y., Zhou, W., Wu, Y., and Huang, Y. (2011). "Bamboo fibers @ poly(ethylene glycol) reinforced poly (butylene succinate) biocomposites," *J. Appl. Polym. Sci.* 122, 2456-2466

Chen, H., Niao, M., and Ding. X. (2009). "Influence of moisture absorbtion on the interfacial strength of bamboo/vinyl ester composites," *Composites Part A* 40, 2013-2019.

Bendahou, A., Habibi, Y., Kaddami, H., and Dufresne, A. (2009). "Physico-chemical characterization of palm from *Phoenix dactylifera* – L, Preparation of cellulose whiskers and natural rubber–based nanocomposites," *J. Biobased Mater. Bioenergy* 3, 81-90.

Boustany, K., and Hamed, P. (1974). "Short cellulosic fibers new reinforces for rubbers," *Rubber World* 171(2), 39-40.

Bras, J., Hassan, M. L., Bruzesse, C., Hassan, E. A., El-Wakil, N. A., and Dufresne, A. (2010). "Mechanical, barrier, and biodegradability properties of bagasse cellulose whiskers reinforced natural rubber nanocomposites," *Industrial Crops and Products* 32, 627-633.

Brydson, J. A. (1978). *Rubber Chemistry*, Springer, London.

Coran, A. Y., Boustany, K., and Hamed, P. (1974). "Short-fiber-rubber composites: The properties of oriented cellulose-fiber-elastomer composites," *Journal of Rubber Chemical Technology* 47(2), 396-410.

Dufresne, A. (2006). "Comparing the mechanical properties of high performances polymer nanocomposites from biological sources," *Nanoscience Nanotechnology* 6, 322-330.

Derringer, C. (1971). "Short fiber-elastomer composites," *Journal of Elastoplastics* 3, 230-248.

Ellis, B., and Welding, G. N. (1964). *Techniques of Polymer Science*, Society of Chemical Industry, London.

Favier, V., Canova, G. R., Cavaillé, J. Y., Chanzy, H., Dufresne, A., and Gauthier, C. (1995). "Nanocomposites materials from latex and cellulose whiskers," *Polymer Advanced Technology* 6, 351-355.

Hajji, P., Cavaille, J. Y., Favier, V., Gauthier, C., and Vigier, G. (1996). "Tensile behavior of nanocomposites from latex and cellulose whiskers," *Polymer Composites* 17, 4-11.

Henriksson, M., and Berglund, L. A. (2007). "Structure and properties of cellulose nanocomposite films containing melamine formaldehyde," *J. Appl. Polym. Sci.* 106, 2817-2824.

Hoffman, W. (1967). *Vulcanization and Vulcanizing Agents*, LacLean, London, England.

Jacob, M., Thomas, S., and Varughese, K. T. (2004). "Mechanical properties of sisal/oilpalm hybrid fiber reinforced natural rubber composites," *Comp. Sci. Technol.* 64, 955-965.

Jonoobi, M., Jalaluddin, H., Mathew A. P., and Oksman, K. (2010). "Mechanical properties of cellulose nanofiber (CNF) reinforced polylactic acid (PLA) prepared by twin screw extrusion," *Compos. Sci. Technol.* 70(12), 1742-1747.

LeVan, S. L. (1989). "Thermal degradation," *Concise Encyclopedia of Wood and Wood-based Materials*, A. P. Scniewind (ed.), Pergamon Press, New York, 271-273.

Nair, K. G., and Dufresne, A. (2003). "Crab shell chitin whisker reinforced natural rubber nanocomposites. 1. Processing and swelling behavior," *Biomacromolecules* 4, 657-665.

Phiriyawirut, M., Chotirat, N., Phromsiri, S., and Lohapaisarn, I. (2010). "Preparation and properties of natural rubber-cellulose microfibril nanocomposite films," *Adv. Mater. Res.* 93-94, 328-331.

Samir, M. A. S. A., Alloin, F., and Dufresne, A. (2005). "Review of recent research into cellulosic whiskers, their properties and their application in nanocomposite field," *Biomacromolecules* 6, 612-626.

Siqueira, G., Abdillahi, H., Bras, J., and Dufresne, A. (2010). "High reinforcing capability cellulose nanocrystals extracted from *Syngonanthus nitens* (Capim Dourado)," *Cellulose* 17(2), 289-298.

Siqueira, G., Tapin-Lingua, S., Bras, J., Perez , D. S., and Dufresne, A. (2011). "Mechanical properties of natural rubber nanocomposites reinforced with cellulosic nanoparticles obtained from combined mechanical shearing, and enzymatic and acid hydrolysis of sisal fibers," *Cellulose* 18, 57-65.

Scurlock, J. M. O., Dayton, D. C., and Hames, B. (2000). "Bamboo: An overlooked biomass resource?" *Biomass Bioenergy* 19, 229-244.

Varghese, S., and Karger-Kocsis, J. (2003). "Natural rubber basednanocomposites by latex compounding with layered silicates," *Polymer* 44 4921-4927.

Visakh, P. M., Thomas, S., Oksman, K., and Mathew, A. P. (2012a). Cellulose nanofibres and cellulose nanowhiskers based natural rubber composites: Diffusion, sorption, and permeation of aromatic organic solvents," *J. Appl. Polym. Sci.* 124, 1614-1623.

Visakh, P. M., Thomas, S., Oksman, K., and Mathew, A. P. (2012b). "Crosslinked natural rubber nanocomposites reinforced with cellulose whiskers isolated from bamboo waste: Processing and mechanical/thermal properties," *Composites Part A*. 43, 735-741.